Microstructure and Particle Size Effects on Fracture in Aluminum Metal Matrix Composites

M. MANOHARAN, C. LIU, and J. J. LEWANDOWSKI
Department of Materials Science and Engineering, Case Western Reserve University, Cleveland, Ohio 44106, USA

ABSTRACT

The deformation and fracture behavior of aluminum alloy metal matrix composites have been studied by systematic variation of the matrix aging treatment and SiC particle size. Heat treatments were designed to produce underaged and overaged microstructures possessing equivalent values of yield strength and matrix microhardness. Mechanical testing was conducted on smooth tensile and smooth bend specimens, in addition to both notched and precracked fracture toughness specimens. It is shown that both the matrix microstructure and the SiC particle size affect the failure micromechanisms. Microstructure and fracture surface analyses were performed using a combination of scanning and transmission electron microscopy. The results are discussed in light of recent work on fracture of composite materials.

KEYWORDS

Aluminum Metal Matrix Composite, SiC Particulate, Interface Effects, Fracture Toughness, Micromechanisms.

INTRODUCTION

Considerable work has recently been devoted to the area of metal matrix composites (MMC) due to the need for materials with high specific strength and stiffness. The desired form of the reinforcement (i.e. filament, fiber, particulate, whisker) depends strongly on the intended use and requirements, with continuous reinforcement offering the highest potential strength and stiffness, but with marked anisotropy. Although the strength and stiffness of discontinuous reinforced composites are somewhat lower than continuous reinforced materials containing equivalent reinforcement levels, the discontinuous reinforced MMC's hold the additional advantages of possessing more isotropic properties (Lewandowski et. al., 1987b), the

potential of being fabricated via powder metallurgy (P/M) or casting techniques (Schuster et. al., 1987), or by conventional metalworking processes such as extrusion, rolling, etc.

Although it is well accepted that microstructural changes exert significant effects on deformation and fracture for both ferrous (Knott, 1973; Lewandowski and Thompson, 1986a) and non-ferrous (Garrett and Knott, 1978; Lewandowski and Knott, 1985) monolithic materials, relatively few studies have focussed on the role(s) of microstructure in the deformation and fracture of MMC's. The microstructure of a composite material, however, consists not only of the matrix aging condition and interface regions, but includes the reinforcement size, size distribution, and volume fraction. Recent studies have demonstrated significant effects of matrix alloy selection (McDanels, 1985) as well as matrix aging condition(Lewandowski et. al., 1987b, 1988) on monotonic fracture properties. As a continuation of our previous work (Lewandowski et. al., 1987b , 1988; Liu et. al., 1988a, 1988b), the present work investigates the effects of matrix aging condition (i.e. matrix temper) and reinforcement particle size on fracture toughness and fracture micromechanisms in a SiC reinforced aluminum alloy.

EXPERIMENTAL PROCEDURE

Materials and Heat Treatment

The powder metallurgy matrix alloy composition used in this work, designated Alcoa MB78, contains 7%Zn, 2%Cu, and 0.14%Zr, balance Al, and was reinforced with 20% by volume of either F-600 grade (average size prior to blending = 13 μm) or F-1000 grade (average size = 5 μm) SiC particulate. Additional details of the processing of this material via powder metallurgy techniques can be found elsewhere (Lewandowski et. al., 1987b; 1988). The as-extruded materials were subsequently solution heat treated at 500°C/4 hrs, cold water quenched, and artificially aged. The aging treatments for the composites were selected to provide equivalent values of matrix microhardness and yield strength in the composite for the underaged (UA) and overaged (OA) conditions. Aging to the underaged (UA) temper was conducted at 120°C/20 minutes, while the overaged (OA) temper was produced by a double aging treatment: 120°C/24 hours, followed by 170°C/36 hours.

Microstructural Evaluation

Quantitative metallographic techniques were utilized to characterize the average SiC particle size and size distribution in the composite. Micrographs obtained on a JEOL-35SM Scanning Electron Microscope (SEM) were analyzed with a Zeiss Videoplan 2 Image Analyzer, while foils for transmission electron microscopy (TEM) examination were prepared using an ion miller equipped with a cold stage.

Mechanical Testing

Tensile testing was performed in the longitudinal orientation on cylindrical tensile specimens with diameter 5 mm and gage length 25.4 mm at a nominal strain rate of 1×10^{-3}/sec on an INSTRON 1125 Universal Testing Machine equipped with special fixturing designed to reduce bending moments. Strain was monitored via an extensometer affixed to the specimen surface.

Bend testing was conducted in four point bending on both smooth and notched bend specimens of nominal dimensions : 12.7 mm x 12.7 mm x 75 mm. The tensile surfaces on the smooth specimens were polished prior to loading so that the surface deformation (i.e. SiC fracture, matrix failure, interface

failure) could be monitored after periodic increments of strain, including the failure strain. The details of notched bend testing have been described elsewhere (Knott, 1973; Lewandowski et. al., 1984, 1986a, 1987a, 1987b) where they have been utilized to examine the fracture initiation details ahead of a blunt stress concentrator. Toughness testing was additionally conducted on bend specimens containing notches of the following root radii: 1.0 mm, 0.25 mm, 0.06 mm, and fatigue precracked specimens. The notches were either ground or introduced via a high speed wire saw, while fatigue precracks were started from one of the geometries. A clip gage was attached to the specimen surface through knife edges for continuous monitoring of the strain.

Fracture Surface Analyses

Fracture surfaces were analyzed using a JEOL 35SM SEM equipped with a PGT Microanalysis System. The fracture surfaces were characterized by performing matching surface fractography, while the area fraction and particle size distributions of SiC present on the fracture surface were quantified. Observations were made at magnifications of 1000X-5000X. Particular emphasis was placed on determining the relative amounts of SiC fracture vs decohesion, as affected by changes in matrix microstructure, while quantification of the data was accomplished with a Zeiss Videoplan 2 equipped with a statistical package.

RESULTS

Microstructures

TEM of the as-extruded material has been reported elsewhere (Lewandowski et. al., 1987b, 1988) while Figs. 1a and 1b illustrate the microstructures of the UA and OA materials, respectively. The UA material did not exhibit precipitates (Fig. 1a), in contrast to the OA material which exhibited extensive precipitation in the matrix as well as particles at the SiC/matrix interfaces, Figure 1b. EDAX analyses revealed that the interface particles contained both Mg and Zn. Diffraction pattern analyses of these interface particles in the OA and in a severely overaged material identified the particles as $MgZn_2$, proving that these particles were neither carbides nor coarse intermetallic particles.

Mechanical Properties

Table 1 summarizes the uniaxial tensile properties for the UA and OA composite materials. Equivalent values of yield strength, reduction of area, and work hardening exponent, n, were obtained for the conditions tested. Also included in Table 1 are the results of quantitative fractography, which reveals a large difference in the amount of fractured SiC present on the fracture surfaces. The UA material containing 13 μm average size SiC (i.e. UA-13μm) exhibited a preference for fracture of the SiC, while the UA-5μm material exhibited a preference for matrix failure and failure near the SiC/matrix interfaces. Both the OA-5μm and OA-13μm materials exhibited a preference for failure near the SiC/matrix interfaces and in the matrix. Figure 2 presents the fracture surfaces for the conditions tested, illustrating larger dimples for the 13 μm material than for the 5 μm material. TEM of foils taken from beneath the fracture surfaces of the two materials (i.e. UA vs OA) corroborated the differences in fracture mode observed, although some fractured SiC were observed in the foils taken from the fractured UA-5μm material.

The surfaces of the smooth bend specimens also revealed an effect of matrix

microstructure on the fracture micromechanisms. The UA-13μm material exhibited both fractured inclusions and fractured SiC near the fracture surface, Fig. 3a, while the UA-5μm material exhibited a smaller proportion of fractured SiC, with additional failure in the matrix and near the SiC/matrix interface, Fig. 3b. Multiple fracture of elongated SiC was also observed for the UA-13μm material, as illustrated in Fig. 3a. OA specimens exhibited preferential failure in the matrix and at the SiC/matrix interfaces, Fig. 3c. Figure 4 presents the size distribution of fractured SiC present on the surfaces of fractured tensile specimens of the UA-13μm material, indicating preferential fracture of the larger SiC. Apart from the fracture surface observations, the smooth bend specimens additionally revealed preferential fracture of elongated particles.

Table 2 summarizes the effect of matrix aging condition, SiC particle size, and notch root radius on the toughness of the composites tested. The UA materials consistently exhibited higher fracture toughnesses compared to the OA materials, although the finer SiC particle size (i.e. 5 μm material) used in this study did not provide any improvement in properties in comparision to the material containing the coarser particle size (i.e. 13 μm material). A notch root radius effect on the calculated toughnesses was also observed for each of the conditions tested. The specimens with notch root radius of 1 mm provided the highest toughness values while decreases in the notch radius produced significant decreases in the calculated toughness values. Specimens with the smallest notch root radius (i.e. 0.06 mm) exhibited toughness values very similar to those obtained in the fatigue precrackd specimens.

DISCUSSION

The tensile specimens exhibited significant differences in fractography between UA and OA materials while possessing equivalent strength and matrix microhardness. A preference for SiC fracture was observed in the UA-13μm specimens, in contrast to the UA-5μm and all the OA specimens which exhibited failure at and near the SiC/matrix interfaces. Intriguingly, the large differences in fractographic details were not reflected in the macroscopic measures of ductility, such as reduction in area (i.e. RA) or fracture strain. Although major effects of matrix microstructure on the failure mechanisms have been presently observed in SiC reinforced 7XXX alloys (Lewandowski et. al., 1987b, 1988) and recently in 6XXX alloys (Voelkel, 1988) reinforced with SiC, other recent work on 2XXX alloys (You et. al., 1987) did not reveal such effects of matrix microstructure on the micromechanisms of failure. Possible sources of these differences may relate to the details of the processing techniques, and/or differences in aging treatments and aging response in the various studies. Coarse intermetallic particles have often been found to initiate failure in materials processed via super-solidus consolidation (Voelkel, 1988; You et. al., 1987). On the other hand, materials processed using sub-solidus consolidation (Lewandowski et. al., 1987b, 1988; Liu et. al., 1988a) often revealed preferential fracture in regions of clustered SiC. The source of these discrepancies may relate to subtle differences in the aging treatments employed in the various works, as well as to possible differences in the aging response of the various alloys. Work is continuing to investigate the possible reasons for the observed differences in fracture behavior between various composites.

As mentioned above, for the present work on 7XXX alloys consolidated below the solidus temperature, both SEM and TEM observations have revealed a preference for SiC fracture in UA-13μm materials, with a preference for interface, or near-interface failure in the OA condition. The smooth bend

specimens provided additional information on the sequence of events leading to catastrophic failure in these composites. Fracture initiation at low strains occurred in the UA-13μm material via fracture of elongated SiC, large SiC, and at inclusions, while multiple fractures in the SiC were observed at higher strains. Fracture in the UA-5μm materials occurred at inclusions, in the large SiC particles, and near the SiC/matrix interfaces. OA specimens similarly revealed fractured inclusions, although subsequent fracture appears to be always dominated by failure near the SiC/matrix interfaces and failure in the matrix, for all particle sizes studied.

Related work on these alloys has revealed that fracture initiation occurs preferentially in regions of clustered SiC (Lewandowski et. al., 1987b; Liu et. al., 1988a) and also demonstrated that the 5 μm material possessed greater clustering of SiC compared to the 13 μm material. These observations may be particularly relevant in the present study on micromechanisms of fracture and fracture toughness. Conventional wisdom for materials containing dispersions of hard particles would suggest an improvement in damage tolerance with a reduction in the particle size for a given strength and volume percent (Broek, 1973). However, Argon, et. al., (1975), have demonstrated that void nucleation processes are not necessarily intrinsic but rather a result of the distribution of local volume fraction. Thus, in regions of high clustering, higher stresses could be acheived. This should facilitate void nucleation at lower macroscopic (i.e. far field) stress levels in these regions. In materials exhibiting a low strain to fracture, as exemplified by the present materials, this phenomenon may become particularly important. Thus, the lack of improvement in fracture toughness with a decrease in the SiC particle size is consistent with the above rationalizations. This approach and the results outlined above suggest the problems associated with an approach based soley on predicting properties based on average particle size and distribution, and emphasizes the need to consider the roles of clustered regions on properties in these complex composites.

Although the macroscopic tensile properties did not reveal a substantial effect of matrix microstructure on yield strength, work hardening exponent (i.e. n), or reduction of area, the fracture toughness values were significantly lower in the OA materials compared to the UA materials. Consistent with this observation, quantitative fractography revealed a preference for SiC fracture in UA-13μm materials, with interface or near-interface failure preferred in OA materials. It should be noted that average particle sizes larger than 13μm (in similar matrix materials) have been shown to produce significantly lower values for notch toughness and short rod toughness (Hunt, 1988) in composites containing levels of reinforcement and microstructures identical to those tested presently.

The present results additionally indicate that interfacial regions may play a dominant role in the fracture behavior of particulate reinforced MMC's. It is shown that interface and near interface failure in OA alloys accompanies a large drop in notch toughness, although the macroscopic tensile properties are relatively unaffected by the aging treatments employed. While few systematic studies have been performed to investigate the details of fracture initiation and propagation in these materials, the present results indicate that both the matrix microstructure (i.e. aging condition, particle size, size distribution) and the details of the reinforcement/matrix interface may exert major effects on the mechanical behavior of these materials. Furthermore, a particle size effect has been observed in the UA material (Lewandowski et. al., 1987b, 1988; Liu et. al., 1988a), whereby large and elongted SiC fractured during testing in preference to the smaller SiC. This observation has been corroborated in the present work via the observed transition from SiC fracture in the

UA-13μm material to failure predominantly in the matrix and near the interface in the UA-5μm material. Similar observations where the fracture path appears to preferentially fracture large particles in a composite material has been reported by Ritter (Ritter, 1987).

CONCLUSIONS

1. Heat treatments have been designed to systematically vary the matrix microstructure and SiC/matrix interface in P/M 7XXX Aluminum alloys reinforced at the 20 volume percent level with either 13 μm or 5 μm SiC particles. Equivalent tensile properties and matrix microhardnesses were obtained for the conditions tested.

2. Despite the relative similarity in macroscopic tensile properties and ductilities between the UA and OA materials, quantitative fractography revealed a preference for SiC fracture in UA-13μm materials, with a predominance of interface or near interface failure in the OA materials and the UA-5μm material. Quantitative fractography also revealed that large SiC are preferentially fractured.

3. Smooth bend specimens sequentially loaded to higher strain levels including failure were successfully used to detail the stages of damage accumulation for the conditions tested. Multiple fracture of individual SiC was often observed for the UA-13μm material, with a preference for failure in the matrix and near the interface in the UA-5μm material. OA materials exhibited preferential failure in the matrix and near the SiC/matrix interfaces.

4. A notch root radius effect on the measured values of toughness was observed for both the UA and OA composites tested.

5. Higher fracture toughness values were obtained in the UA materials compared to the OA materials. No improvement in properties were obtained in the material containing the finer SiC particles.

ACKNOWLEDGEMENTS

The authors would like to thank W.H. Hunt, Jr. of ALCOA Laboratories for the supply of material and the provision of a one-year fellowship for one of the authors (CL). Additional support has been supplied by an AIME Research Initiation Grant (JJL) with experimental support from DARPA-ONR-N00014-86-K-077

REFERENCES

Argon, A.S. (1975). Met. Trans. A, 6A, 825-837.
Broek, D. (1973). Engineering Fracture Mechanics, 5, 55-66.
Garrett, G.G. and J.F. Knott (1978). Met. Trans. A, 9A, 1187-1201.
Hunt, W.H. Jr. (1988). Personal Communication.
Knott, J.F. (1973). Fundamentals of Fracture Mechanics, Butterworths.
Lewandowski, J.J. and A.W. Thompson (1984). In: Proc. ICF6 (S.R. Valluri, et al, eds.), Vol. 2, pp. 1515-1524. Pergamon, Oxford.
Lewandowski, J.J. and J.F. Knott (1985). In: Proc. ICSMA-7 (H. McQueen, et al, eds.), Vol. 2, pp. 1193-1199. Pergamon, Oxford.
Lewandowski, J.J. and A.W. Thompson (1986a). Met. Trans. A, 17A, 461-472.
Lewandowski, J.J. and A.W. Thompson (1986b). Met. Trans. A, 17A, 1769-1786.
Lewandowski, J.J., C.A. Hippsley and J.F. Knott (1987a). Acta Met., 35, 593-608.
Lewandowski, J.J., C. Liu and W.H. Hunt, Jr. (1987b). In: Powder Metallurgy Composites (M. Kumar, K. Vedula, and A.M. Ritter, eds.), pp. 117-137, TMS-AIME, Warrendale, PA.

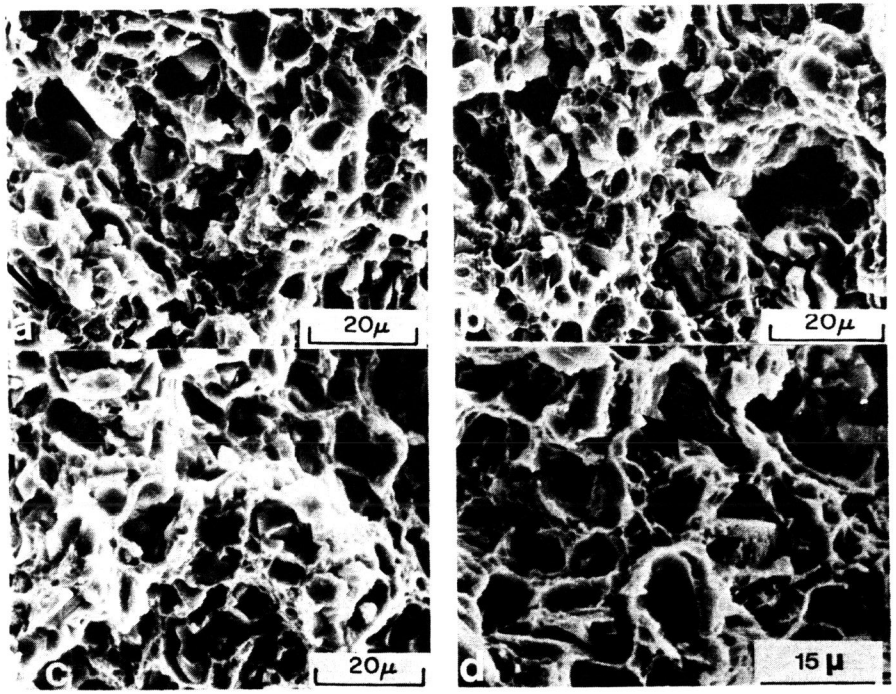

Fig. 2 SEM fractographs of UA and OA materials containing either 5 μm or 13 μm SiC: a) UA-5μm, b) OA-5μm, c)UA-13μm, d)OA-13μm.

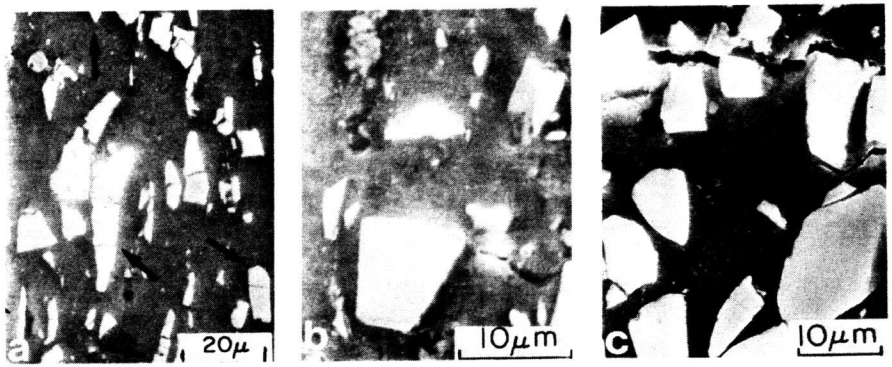

Fig. 3 SEM views of surfaces of smooth bend specimens strained to failure.
a) UA-13μm - Multiple fracture of SiC observed.
b) UA-5μm - Matrix and near interface failure observed.
c) OA-13μm - Matrix and near interface failure observed.

Lewandowski, J.J., C. Liu and W.H. Hunt, Jr. (1988). Mat. Sci. and Eng. in press
Liu, C., S. Pape and J.J. Lewandowski (1988a). In: Proc. ICCI-II (H. Ishida, ed.), pp. 513-25, Elsevier, New York, New York.
Liu, C. and J.J. Lewandowski (1988b), In: Proc. Conf. on Advanced Structural Materials (D. Wilkinson and D.J. Lloyd, eds.), Can. Inst. Metals, in press.
McDanels, D.L. (1985). Met. Trans. A, 16A, 1105-1115.
Ritter, A.M. (1987). In: Powder Metallurgy Composites (M. Kumar, K. Vedula and A.M. Ritter, eds.), pp. 59-79, TMS-AIME, Warrendale, PA.
Schuster, D.M., M. Skibo and F. Yep (1987). J. Met., 39, 60.
Voekel, A. (1988) Unpublished Results, Carnegie-Mellon University.
You, C.P., A.W. Thompson and I.M. Bernstein (1987). Scripta Met., 21, 181-185.

Table 1. Mechanical Properties of Composites Tested.

MATERIAL	σ_y (MPa)	UTS (MPa)	n	% RA	% Surface Covered by Fractured SiC
UA-13μm	381	502	0.16	7.7	18
OA-13μm	406	460	0.16	7.4	11
UA-5 μm	379	496	N/A	8.3	12
OA-5 μm	418	470	N/A	7.3	10

Table 2. Effects of Microstructure and Notch Radius on Toughness. ($MPa\sqrt{m}$)

MATERIAL	NOTCH ROOT RADIUS			
	1.0 mm	0.25 mm	0.06 mm	Fatigue Precracked
UA-13μm	55.4	39.3	25.5	24.2
OA-13μm	34.4	22.2	16.5	17.0
UA-5 μm	N/A	N/A	24.0	N/A
OA-5 μm	N/A	N/A	15.0	N/A

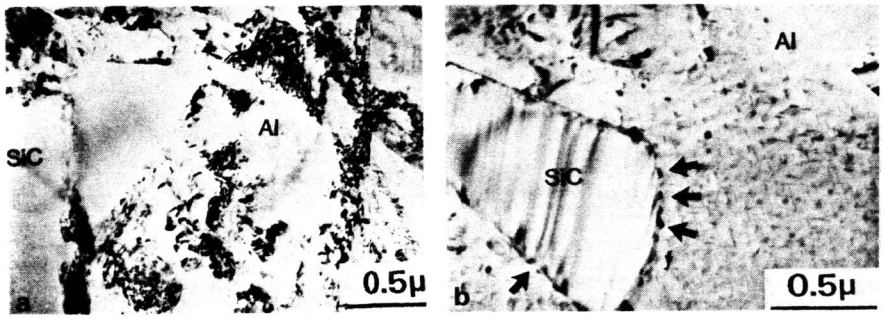

Fig. 1 TEM micrographs of the a) UA and b) OA composites.

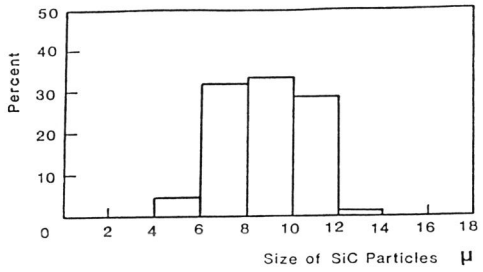

Fig. 4 Size distribution of cracked SiC present on fracture surface of UA-13μm material.